The Eleventh International Conference on
Engineering Computational Technology
23–25 August, 2022 | Montpellier, France

Proceedings of the Eleventh International Conference on
Engineering Computational Technology
Edited by B.H.V. Topping and P. Iványi
Civil-Comp Conferences, Volume 2, Paper 5.8
Civil-Comp Press, Edinburgh, United Kingdom, 2022, doi: 10.4203/ccc.2.5.8


# Static and free vibration analysis of Anisotropic Shells employing Higher Order Shear Deformation Theories and Generalized Differential Quadrature Method

**F. Tornabene, M. Viscoti and R. Dimitri**

**Department of Innovation Engineering**
**University of Salento, Italy**

## Abstract

In the present contribution, a static and a free vibration analysis of anisotropic doubly-curved shells is performed employing higher order theories according to the Equivalent Single Layer (ESL) approach. A unified formulation is adopted for the description of the field variable, and the geometry of the structure is described by means of a set of curvilinear principal coordinates within the reference surface. The fundamental governing equations are derived from the Hamiltonian Principle, and both natural and non-conventional boundary conditions are enforced to the model. General distributions of external surface loads are applied to the structure. The numerical implementation of the differential problem is performed directly in the strong form via the Generalized Differential Quadrature (GDQ). The model is validated with success from a comparison several refined three-dimensional solutions developed with commercial packages. Furthermore, sensitivity analyses outline the influence of the main governing parameters on the static and dynamic structural response.

**Keywords:** anisotropic shells, equivalent single layer, generalized differential quadrature method, higher order theories

# 1 Introduction

Anisotropic materials are very frequently used in many engineering applications where structures of complex shapes are adopted. In this perspective, new efficient computational methodologies are required so that very accurate results are carried out with a reduced computational cost [1].

Two-dimensional Equivalent Single Layer (ESL) formulations can predict with a good level of accuracy the three-dimensional response of doubly-curved structures if a higher order through-the-thickness expansion is adopted to describe the field variable. In this way, an efficient reduction of the material properties to the shell reference surface is essential, especially when lattice materials with a softcore behaviour can be found [2-3].

On the other hand, a Layer-Wise (LW) implementation of the structural problem provides best results for thick shells since the fundamental governing equations are solved within each lamina of laminates, and the compatibility conditions are fulfilled at the interlaminar level [4]. In this way, the geometric description of the structure employing a generalized approach is a key aspect so that structures with zero, single and double curvatures can be embedded in a unified framework. For arbitrarily-shaped shell structures, a distortion of the physical domain is required. Different loads can be applied to the intrados and extrados of the structure, accounting for both smooth distributions and concentrated loads.

The fundamental governing equations, derived from the well-known Hamiltonian Principle, can be numerically tackled following different approaches, such as the domain decomposition methods and spectral collocation procedures. In this contribution, the Generalized Differential Quadrature (GDQ) method is applied for the solution of the structural problem directly in the strong form, together with the implementation of boundary conditions [5-6].

Doubly-curved shell structures are investigated in a comprehensive way, accounting for a generally anisotropic linear elastic constitutive relationship within each lamina. Both ESL and LW solutions are provided, accounting for different numbers of laminae and general material orientations. Furthermore, efficient algorithms are provided for the homogenization of lattice cores. An efficient strategy is adopted for the assessment of natural boundary conditions and non-conventional external constraints, accounting for a generalized distribution of linear elastic springs along the shell edges.

A series of validating examples are presented, in which the static and dynamic response of anisotropic laminated structures with different curvatures is investigated. The numerical predictions are compared to those provided by refined three-dimensional finite element models, showing a very good agreement between different approaches. The present ESL method can predict the three-dimensional response of structures of single and double curvatures employing a reduced computational effort. The present structural theory has been implemented in the package DiQuMASPAB [7], accounting for a higher order implementation of anisotropic doubly-curved shells.

## 2 Methods

According to the ESL approach, a doubly-curved shell structure can be described starting from its reference surface $\mathbf{r}(\alpha_1,\alpha_2)$, whose parametric equation is written in principal coordinates. If we denote with $\mathbf{R}(\alpha_1,\alpha_2,\zeta)$ the generic position vector of a doubly-curved structure, one gets:

$$\mathbf{R}(\alpha_1,\alpha_2,\zeta)=\mathbf{r}(\alpha_1,\alpha_2)+\frac{h(\alpha_1,\alpha_2)}{2}z\mathbf{n}(\alpha_1,\alpha_2) \tag{1}$$

where $h(\alpha_1,\alpha_2)$ stands for the shell thickness, whereas $z=2\zeta/h$ is a dimensionless coordinate for the identification of the points alongside the normal direction $\mathbf{n}(\alpha_1,\alpha_2)$. Starting from Eqn. (1), a unified approach is adopted for the description of the field variable, taking in account a proper set $\mathbf{F}^{(k\tau)}(\zeta)$ of generalized thickness functions, referred to a generic $\tau$-th kinematic expansion order. The three-dimensional displacement field vector $\mathbf{U}^{(k)}(\alpha_1,\alpha_2,\zeta,t)=\left[U_1^{(k)}\ U_2^{(k)}\ U_3^{(k)}\right]^T$ can be thus expressed as:

$$\mathbf{U}^{(k)}(\alpha_1,\alpha_2,\zeta,t)=\sum_{\tau=0}^{N+1}\mathbf{F}^{(k\tau)}(\zeta)\mathbf{u}^{(\tau)}(\alpha_1,\alpha_2,t) \tag{2}$$

being $\mathbf{u}^{(\tau)}(\alpha_1,\alpha_2,t)$ the generalized displacement field vector referred to each $\tau=0,...,N+1$, lying on the shell reference surface. From the proper selection of $\mathbf{F}^{(k\tau)}(\zeta)$, a series of three-dimensional deflection issues can be effectively described. If a laminated structure composed by $l$ laminae is considered, each $k$-th layer of the stacking sequence, with $k=1,...,l$, can be assumed as a generally anisotropic continuum, whose three-dimensional constitutive relationship between stress and strain vectors $\boldsymbol{\sigma}^{(k)}$ and $\boldsymbol{\varepsilon}^{(k)}$ reads as follows:

$$\boldsymbol{\sigma}^{(k)}=\overline{\mathbf{E}}^{(k)}\boldsymbol{\varepsilon}^{(k)} \quad\leftrightarrow\quad \begin{bmatrix}\sigma_1^{(k)}\\ \sigma_2^{(k)}\\ \tau_{12}^{(k)}\\ \tau_{13}^{(k)}\\ \tau_{23}^{(k)}\\ \sigma_3^{(k)}\end{bmatrix}=\begin{bmatrix}\overline{E}_{11}^{(k)} & \overline{E}_{12}^{(k)} & \overline{E}_{16}^{(k)} & \overline{E}_{14}^{(k)} & \overline{E}_{15}^{(k)} & \overline{E}_{13}^{(k)}\\ \overline{E}_{12}^{(k)} & \overline{E}_{22}^{(k)} & \overline{E}_{26}^{(k)} & \overline{E}_{24}^{(k)} & \overline{E}_{25}^{(k)} & \overline{E}_{23}^{(k)}\\ \overline{E}_{16}^{(k)} & \overline{E}_{26}^{(k)} & \overline{E}_{66}^{(k)} & \overline{E}_{46}^{(k)} & \overline{E}_{56}^{(k)} & \overline{E}_{36}^{(k)}\\ \overline{E}_{14}^{(k)} & \overline{E}_{24}^{(k)} & \overline{E}_{46}^{(k)} & \overline{E}_{44}^{(k)} & \overline{E}_{45}^{(k)} & \overline{E}_{34}^{(k)}\\ \overline{E}_{15}^{(k)} & \overline{E}_{25}^{(k)} & \overline{E}_{56}^{(k)} & \overline{E}_{45}^{(k)} & \overline{E}_{55}^{(k)} & \overline{E}_{35}^{(k)}\\ \overline{E}_{13}^{(k)} & \overline{E}_{23}^{(k)} & \overline{E}_{36}^{(k)} & \overline{E}_{34}^{(k)} & \overline{E}_{35}^{(k)} & \overline{E}_{33}^{(k)}\end{bmatrix}\begin{bmatrix}\varepsilon_1^{(k)}\\ \varepsilon_2^{(k)}\\ \gamma_{12}^{(k)}\\ \gamma_{13}^{(k)}\\ \gamma_{23}^{(k)}\\ \varepsilon_3^{(k)}\end{bmatrix} \quad \text{for} \quad k=1,...,l \tag{3}$$

where $\overline{\mathbf{E}}^{(k)}=\mathbf{T}^{(k)}\mathbf{E}^{(k)}\left(\mathbf{T}^{(k)}\right)^T$ denotes the rotated stiffness matrix of the material. For the sake of completeness, is the rotation matrix $\mathbf{T}^{(k)}$ accounts for the material orientation $\vartheta^{(k)}$ with respect to $\alpha_1$ curvilinear direction, whereas $\mathbf{E}^{(k)}$ is the three-dimensional stiffness matrix written in the material reference system [7]. One gets:

$$\mathbf{E}^{(k)} = \begin{bmatrix} E_{11}^{(k)} & E_{12}^{(k)} & E_{16}^{(k)} & E_{14}^{(k)} & E_{15}^{(k)} & E_{13}^{(k)} \\ E_{12}^{(k)} & E_{22}^{(k)} & E_{26}^{(k)} & E_{24}^{(k)} & E_{25}^{(k)} & E_{23}^{(k)} \\ E_{16}^{(k)} & E_{26}^{(k)} & E_{66}^{(k)} & E_{46}^{(k)} & E_{56}^{(k)} & E_{36}^{(k)} \\ E_{14}^{(k)} & E_{24}^{(k)} & E_{46}^{(k)} & E_{44}^{(k)} & E_{45}^{(k)} & E_{34}^{(k)} \\ E_{15}^{(k)} & E_{25}^{(k)} & E_{56}^{(k)} & E_{45}^{(k)} & E_{55}^{(k)} & E_{35}^{(k)} \\ E_{13}^{(k)} & E_{23}^{(k)} & E_{36}^{(k)} & E_{34}^{(k)} & E_{35}^{(k)} & E_{33}^{(k)} \end{bmatrix} \quad (4)$$

From the computation of the elastic strain energy, the kinetic energy, and the virtual work of external loads within the Hamiltonian Principle, the fundamental set of the governing equations can be derived for each $\tau$-th kinematic expansion order, as follows:

$$\sum_{\eta=0}^{N+1} \mathbf{L}^{(\tau\eta)}\mathbf{u}^{(\eta)} - \sum_{\eta=0}^{N+1} \mathbf{M}^{(\tau\eta)}\ddot{\mathbf{u}}^{(\eta)} + \mathbf{q}^{(\tau)} = 0 \qquad \text{for } \tau = 0,...,N+1 \quad (5)$$

being $\mathbf{L}^{(\tau\eta)}$ the fundamental matrix and $\mathbf{M}^{(\tau\eta)}$ the generalized inertial matrix. External loads $q_1^{(\pm)}, q_2^{(\pm)}, q_3^{(\pm)}$ applied at $\zeta = \pm h/2$, respectively, are embedded in the model once they are reduced to the reference surface with the vector $\mathbf{q}^{(\tau)}$, with $\tau = 0,...,N+1$. The numerical implementation is performed employing the GDQ method, which provides a discretization of the derivative of a generic $n$-th order as a weighted sum of the values assumed by an unknown function $f$ in a pre-determined set of $I_Q$ discrete points. Referring to the one-dimensional case, it gives:

$$f^{(n)}(x_i) = \left.\frac{\partial^n f(x)}{\partial x^n}\right|_{x=x_i} \cong \sum_{j=1}^{I_Q} \varsigma_{ij}^{(n)} f(x_j) \qquad i = 1, 2,..., I_Q \quad (6)$$

being $x_i$ the generic point of the adopted computational grid, whereas $\varsigma_{ij}^{(n)}$ are the weighting coefficients calculated with a recursive procedure. In the same way, the numerical integrations employed in the computation of the components of $\mathbf{L}^{(\tau\eta)}$ are performed with the Generalized Integral Quadrature (GIQ) method, reading as:

$$\int_{x_i}^{x_j} f(x)\,dx = \sum_{k=1}^{I_Q} w_k^{ij} f(x_k) \quad (7)$$

where $w_k^{ij}$ are the GIQ weighting coefficients.

## 3 Results

We present a series of examples where the accuracy of the present formulation is outlined. Three-dimensional finite element solutions have been adopted as a reference results. Structures with different curvatures, thickness variations and lamination schemes have been considered. For each case, vibration frequencies have been evaluated, and the influence of the selection of the thickness functions within the model have been outlined. Furthermore, the static deflection has been considered for a comprehensive set of case studies, and various load distributions have been applied.

When higher order theories are considered, the stretching effect is well predicted by the model. Furthermore, the proposed model is suitable for the prediction of complex interlaminar effects, especially for softcore layers. We report some simulations performed on a fully-clamped ellipsoid. According to Eqn. (1), the reference surface equation, expressed in principal coordinates, reads as:

$$\mathbf{r}(\alpha_1,\alpha_2)=\left(\frac{a\sqrt{a^2-b^2\sin^2\alpha_1-c^2\cos^2\alpha_1}}{\sqrt{a^2-c^2}}\cos\alpha_2\right)\mathbf{e}_1+\left(b\cos\alpha_1\sin\alpha_2\right)\mathbf{e}_2+ \\ +\left(-\frac{c\sqrt{a^2\sin^2\alpha_2+b^2\cos^2\alpha_2-c^2}}{\sqrt{a^2-c^2}}\sin\alpha_1\right)\mathbf{e}_3 \tag{8}$$

setting $a=3$ m, $b=1.5$ m and $c=1$ m. Accordingly, $\mathbf{r}(\alpha_1,\alpha_2)$ has been defined so that $(\alpha_1,\alpha_2)\in[\alpha_1^0,\alpha_1^1]\times[\alpha_2^0,\alpha_2^1]$, where $\alpha_1^0=0$, $\alpha_1^1=\pi$, $\alpha_2^0=\pi/6$ and $\alpha_2^1=5\pi/6$. The structure is made of three layers of triclinic material $\left(\rho^{(k)}=7750\ \mathrm{kg/m^3}\right)$, being $(0/30/45)$ and $h_1=h_2=h_3=0.035\,\mathrm{m}$. The triclinic material is characterized by the following stiffness matrix:

$$\mathbf{E}^{(k)}=\begin{bmatrix} 98.84 & 53.92 & 0.03 & 1.05 & -0.1 & 50.78 \\ 53.92 & 99.19 & 0.03 & 0.55 & -0.18 & 50.87 \\ 0.03 & 0.03 & 22.55 & -0.04 & 0.25 & 0.02 \\ 1.05 & 0.55 & -0.04 & 21.1 & 0.07 & 1.03 \\ -0.1 & -0.18 & 0.25 & 0.07 & 21.14 & -0.18 \\ 50.78 & 50.87 & 0.02 & 1.03 & -0.18 & 87.23 \end{bmatrix}\ \mathrm{GPa} \tag{9}$$

In Table 1 the first ten mode frequencies have been reported. The GDQ solution has been calculated with a Chebyshev-Gauss-Lobatto grid [6] with $I_N=I_M=31$. When higher order theories are adopted, the results perfectly match those of a refined 3D FEM model with C3D20 parabolic brick elements, especially when the zigzag functions are adopted in Eqn.(2). In Figure 1 we report the first nine mode shapes of the structure calculated with the EDZ4 theory. A uniform surface load equal to $q_3^{(+)}=-5000\,\mathrm{N}$ has been then applied to the structure, and the static response of the ellipsoid has been calculated with the higher order formulation of Eqn. (5). The three-dimensional static behaviour along the thickness of the shell has been derived at $\left(0.25(\alpha_1^1-\alpha_1^0),0.25(\alpha_2^1-\alpha_2^0)\right)$. Different higher order theories have been adopted, as well as classical FSDT and the TSDT theories [6]. In Figure 2 the distributions of the displacement components have been calculated from Eqn. (2), whereas in Figures 3-4 the stress and strain components have been evaluated from the recovery procedure outlined in Ref. [7].

| Ellipsoid (CCCC) | | | | | | | | | |
|---|---|---|---|---|---|---|---|---|---|
| **Mode** $f\,[\mathrm{Hz}]$ | **3D FEM** | **FSDT** | **TSDT** | **ED2** | **EDZ2** | **ED3** | **EDZ3** | **ED4** | **EDZ4** |
| **DOFs** | 601317 | 5046 | 10092 | 7569 | 10092 | 10092 | 12615 | 12615 | 15138 |
| 1 | 107.02 | 107.10 | 107.10 | 106.99 | 106.95 | 107.01 | 107.01 | 107.00 | 107.00 |
| 2 | 111.09 | 111.04 | 111.05 | 110.96 | 110.83 | 111.03 | 111.02 | 111.00 | 111.00 |
| 3 | 158.18 | 158.25 | 158.26 | 158.07 | 157.93 | 158.14 | 158.14 | 158.12 | 158.12 |
| 4 | 177.50 | 177.52 | 177.54 | 177.35 | 177.17 | 177.47 | 177.47 | 177.45 | 177.45 |
| 5 | 181.62 | 181.23 | 181.26 | 181.26 | 180.88 | 181.47 | 181.46 | 181.41 | 181.40 |
| 6 | 201.67 | 201.79 | 201.80 | 201.55 | 201.39 | 201.65 | 201.64 | 201.63 | 201.63 |
| 7 | 228.52 | 228.49 | 228.52 | 228.25 | 227.94 | 228.47 | 228.47 | 228.44 | 228.44 |
| 8 | 233.14 | 232.44 | 232.50 | 232.57 | 232.00 | 232.97 | 232.96 | 232.90 | 232.89 |
| 9 | 242.28 | 242.37 | 242.39 | 242.10 | 241.89 | 242.25 | 242.24 | 242.23 | 242.22 |
| 10 | 255.05 | 254.86 | 254.89 | 254.80 | 254.51 | 255.00 | 255.00 | 254.98 | 254.98 |
| **Geometric Inputs:** $a = 3$ m, $b = 1.5$ m, $c = 1$ m; $\alpha_1^0 = 0$, $\alpha_1^1 = \pi$, $\alpha_2^0 = \pi/6$ and $\alpha_2^1 = 5\pi/6$ | | | | | | | | | |

Table 1: Free vibration analysis of a fully-clamped ellipsoid laminated with generally anisotropic materials employing higher order theories.

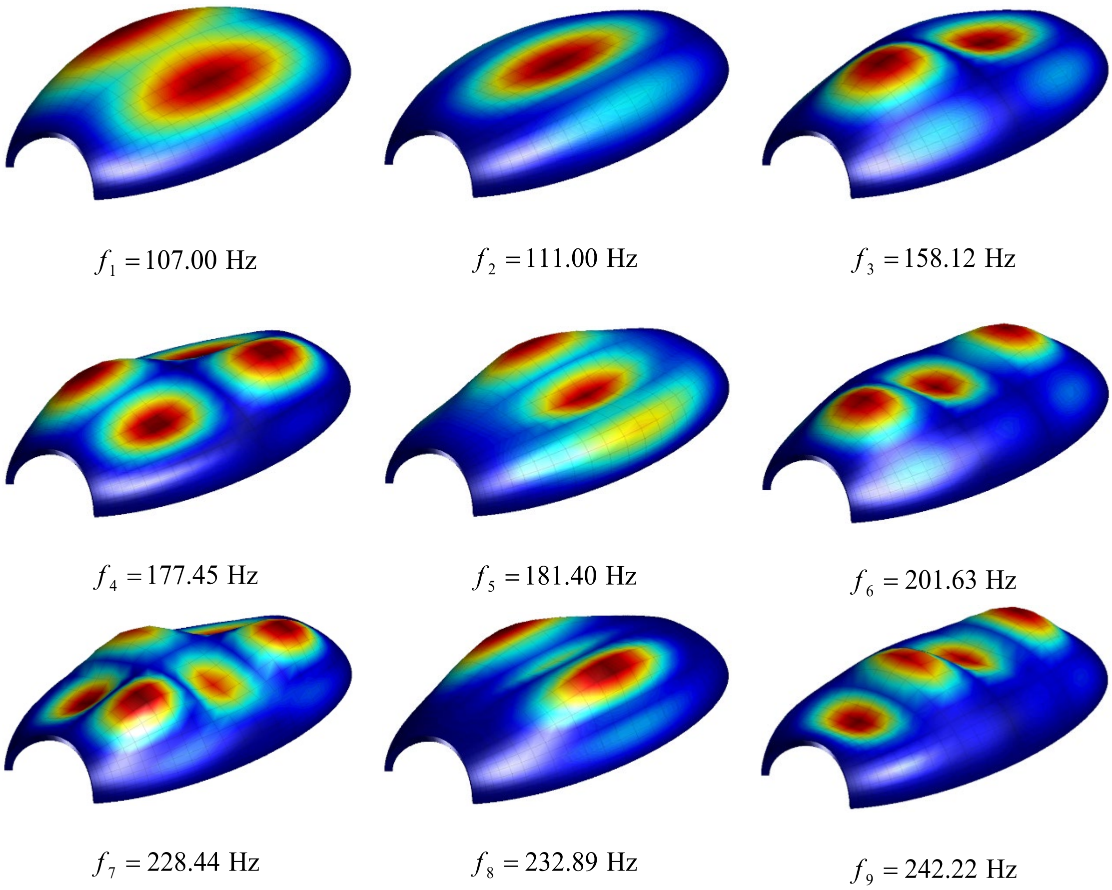


Figure 1: First nine mode shapes of a fully-clamped ellipsoid laminated with generally anisotropic materials employing the EDZ4 theory.

As can be seen, classical ESL approaches are not capable of providing the out-of-plane stretching effects, whereas a higher order assumption is capable of well predicting the out-of-plane response of the structure. Furthermore, only a higher order assumption for the out-of-plane displacement field component can predict the through-the-thickness stretching effect. As a matter of fact, the stress distribution perfectly fulfils the equilibrium conditions due to the application of external loads.

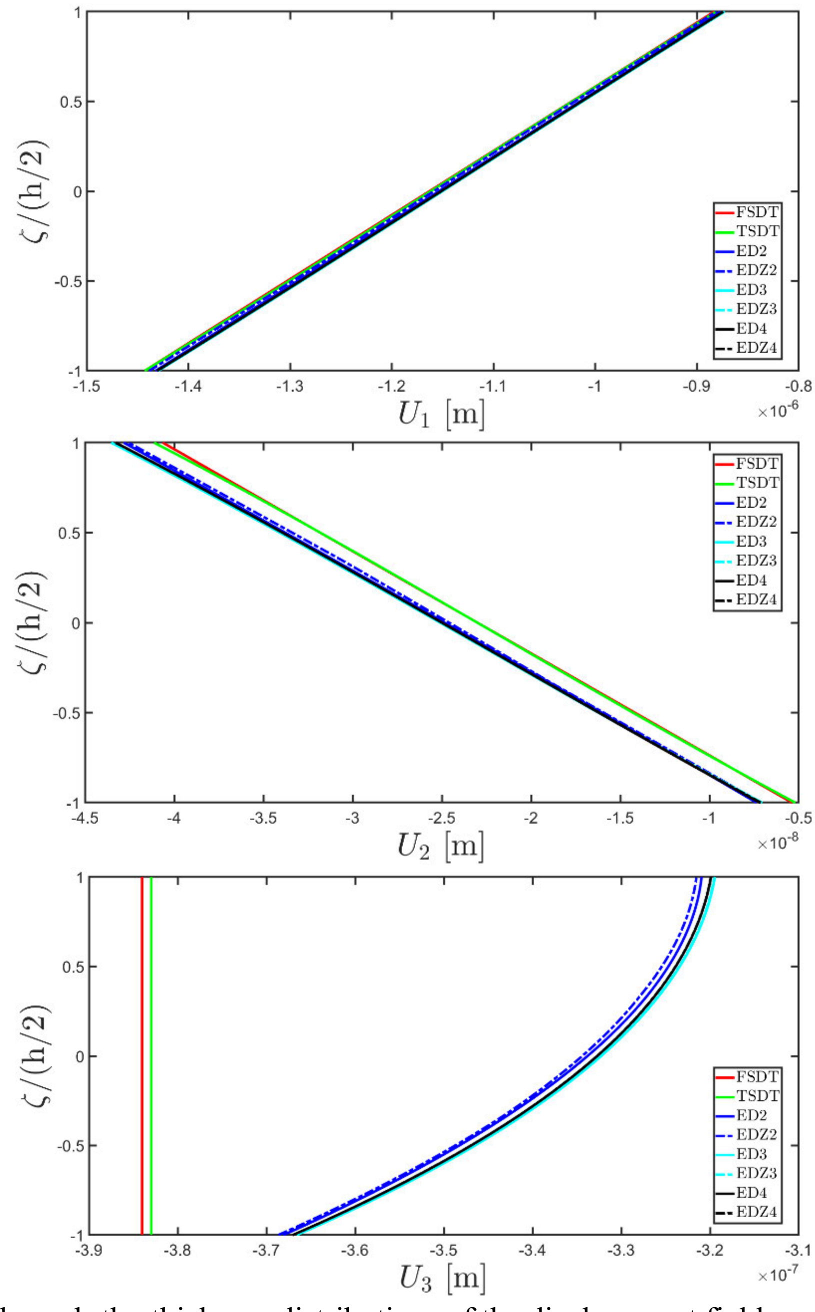


Figure 2: Through-the-thickness distributions of the displacement field components calculated by means of various higher order ESL theories of a fully-clamped ellipsoid subjected to a uniform surface load applied at the top surface.

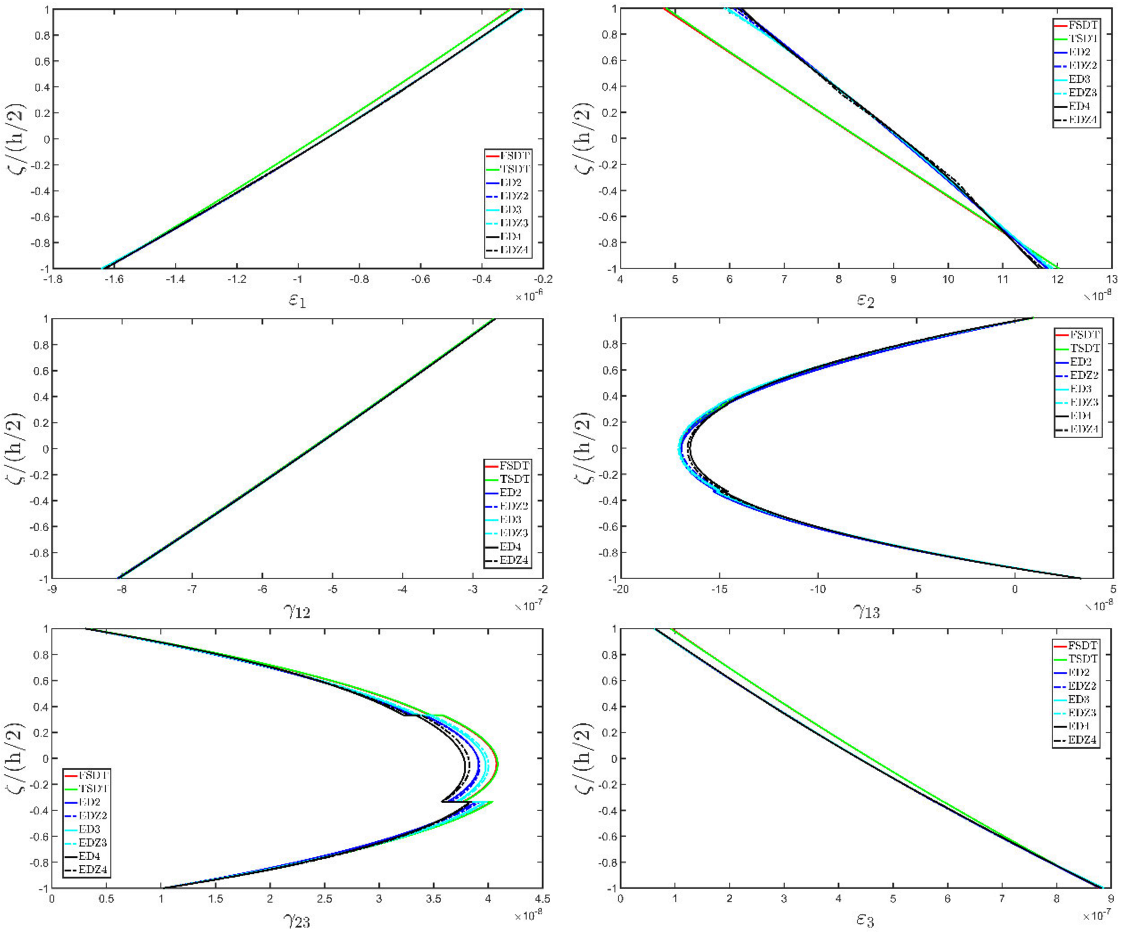

Figure 3: Through-the-thickness distributions of the three-dimensional strain components calculated by means of various higher order ESL theories of a fully-clamped ellipsoid subjected to a uniform surface load applied at the top surface.

# 4 Conclusions and Contributions

In the present contribution, some higher order theories have been adopted in a generalized two-dimensional formulation for the static and free vibration analysis of laminated anisotropic doubly-curved shells. The field variable has been described employing a unified formulation, and a curvilinear set of principal coordinates have been adopted for the geometric description of the structures. A mapping procedure has been also adopted for the distortion of arbitrarily-shaped structures, and a rectangular computational domain has been obtained. The fundamental equations and the boundary conditions have been numerically tackled in the strong form with the GDQ method, thus avoiding the employment of pre-determined set of shape functions. An in-plane and an out-of-plane general distribution of linear elastic springs have been applied at the shell edges, and non-conventional boundary conditions have been enforced to the structure. Furthermore, at the top and the bottom surfaces of the shell general distributions of loads have been applied, and an efficient methodology has been followed for the assessment of concentrated loads. Static and dynamic responses of different kind of structures have been investigated, and the results have been compared with success with those provided by other trustworthy formulations. Very accurate results have been obtained with a significantly reduced computational cost.

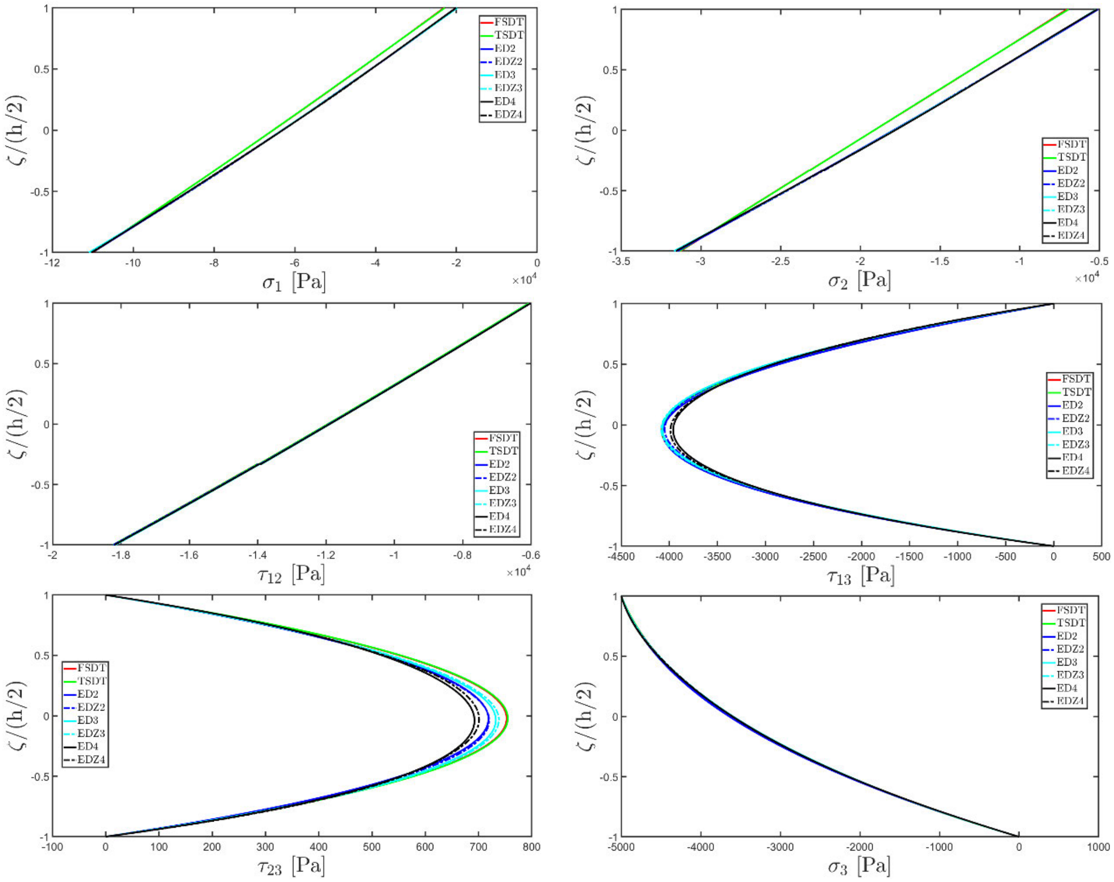


Figure 4: Through-the-thickness distributions of the three-dimensional stress components calculated by means of various higher order ESL theories of a fully-clamped ellipsoid subjected to a uniform surface load applied at the top surface.

# References


[1] Tornabene F., Viscoti M., Dimitri R., Reddy J.N., Higher order theories for the vibration study of doubly-curved anisotropic shells with a variable thickness and isogeometric mapped geometry, Composite Structures, 267 (2021), 113829.

[2] Tornabene F., Viscoti M., Dimitri R., Aiello M.A., Higher-order modeling of anisogrid composite lattice structures with complex geometries, Engineering Structures, 244 (2021), 112686.

[3] Tornabene F., Viscoti M., Dimitri R., Aiello M.A., Higher order formulations for doubly-curved shell structures with a honeycomb core, Thin-Walled Structures, 164 (2021), 107789.

[4] Tornabene F., Viscoti M., Dimitri R. Generalized higher order layerwise theory for the dynamic study of anisotropic doubly-curved shells with a mapped

geometry, Engineering Analysis with Boundary Elements, 134 (2022), 147-183.
[5] Arefi M., Bidgoli E.M.R., Dimitri R., Bacciocchi M., Tornabene F., Nonlocal bending analysis of curved nanobeams reinforced by graphene nanoplatelets, Composites Part B: Engineering, 166 (2019), 1-12.
[6] Tornabene F., Bacciocchi M., Anisotropic Doubly-Curved Shells. Higher-Order Strong and Weak Formulations for Arbitrarily Shaped Shell Structures, Esculapio, Bologna, 2018.
[7] Tornabene F., Fantuzzi N., Bacciocchi M., DiQuMASPAB: Differential Quadrature for Mechanics of Anisotropic Shells, Plates, Arches and Beams, Esculapio, Bologna, 2018.